Proceeding of the Korean Nuclear Society Fall Meeting
Seoul, Korea, October 1998

Development of the Integrated Core On-line Monitoring and Protection Aid Surveillance System

Byung-Oh Cho, Wang Kee In, Jae-Seung Song and Sung-Quun Zee
Korea Atomic Energy Research Institute

Abstract

The integrated Core On-line Monitoring and Protection Aid Surveillance System (COMPASS) is developed for the purpose of supporting the reactor operation, based on the three-dimensional nodal design code, MASTER. The heart of COMPASS is an adaptive nodal core simulator for the on-line calculation of three-dimensional assembly and pin power distributions which are used for the evaluation of the thermal margins and for the guide in operation. In this paper, the overall structures and the solution methods of COMPASS are described. The uncertainty of COMPASS for SMART core was also evaluated by comparing that of MASTER. The results showed that COMPASS uncertainty in power shape prediction is identical to that of the design code system, MASTER. The application of COMPASS to the analysis of peaking factor for SMART core resulted with about 4% gain in peaking factor margin when compared to COLSS.

1. Introduction

There is an increased demand for more and improved software and hardware support for the on-line analysis of the pressurized water reactor (PWR) core for a safe and economical operation. Maintaining a nuclear power plant within its Limiting Conditions for Operation (LCOs) is necessary condition for safe operation and acceptable transient consequences. These LCOs are delineated in the Technical Specifications. There are many systems in a nuclear power plant that are used to help the operators maintain the plant within the LCOs.

For the on-line monitoring and surveillance for the digital CE-plants, COLSS (Core Operating Limit Supervisory System)[1] has been operated for many years. COLSS was developed in a simplified and conservative way due to the immature computer system and technology in 1970's. Since it adopted a very simple numerical solution models for the on-line operation, it unavoidably resulted in excessively conservative thermal margins which degrade plant operation economy. In recent years, by virtue of the computer technology we can obtain high operation performance which was partly impossible in the past due to computing time requirements for power distribution evaluation.

Based on the self-reliance in the commercial PWR design and construction technology in Korea, KAERI is developing System-integrated Modular Advanced ReacTor (SMART) of 330 MWt for supplying the energy for sea water desalination as well as for electricity generation[2]. As a part of the digital safety instrumentation and control system of SMART the integrated Core On-line Monitoring and Protection Aid Surveillance System (COMPASS) is developed on the basis of the COPS (COre Protection and Surveillance)[3] system. The heart of COMPASS is an adaptive nodal core simulator for the on-line calculation of three-dimensional assembly and pin power distributions. The main results of the on-line adaptation procedure are the fluxes, which are optimally adapted to the incore detector measurements and the model parameters (cross sections) adjusted to reproduce

this adapted flux map. These model parameters are then used in the on-line three-dimensional core analysis.

The goal of this paper is to describe the solution methods and the power prediction uncertainty of COMPASS. The solution methods are outlined in section II. In section III, system uncertainty results are presented. This is followed by conclusions of this report in section IV.

II. Solution Methods of COMPASS

The adaptive procedure within COMPASS is described as the following. First, the adaptive simulator of COMPASS converts incore detector readings into local box average fluxes using detailed three-dimensional, two-group diffusion theory calculation imported from the design code, MASTER[4] and Kalman filter techniques[3,5]. These are provided for the instrumented nodes in the core. A core-wide box average flux distribution is then obtained through the use of calculated spatial flux coupling coefficients[6], which relate the fluxes in the instrumented nodes to those in the noninstrumented nodes. Model parameters such as fast and thermal absorption production cross sections are then adjusted in each core node such that the given flux map of average fluxes derived from the process is reproduced.

2.1 Incore Detector Signal Adaptation

The on-line evaluation of the fixed incore detector signals determines the optimal node average fluxes in the instrumented nodes by use of Kalman filter technique and detailed three-dimensional, two-group nodal calculation.

Kalman filter can be regarded as an extension of the Gaussian method of the least mean squares to stochastic processes. The task is to estimate a system variable x (optimal node average fluxes) from a measured signal z (detector signals) where the system variable itself might not be directly measurable. The detailed Kalman filter theory is not presented here. Instead, the final Kalman filter equation for the optimal node average fluxes from the detector signals and the calculated fluxes from the nodal solution is summarized.

$$\hat{\phi}_g^i = \phi_{g,cal}^i + K_g^i \left(A_{g,m}^i - \sum_{g'=1}^{2} H_{g'}^i \phi_{g',cal}^i \right) \quad (1)$$

where

$\hat{\phi}_g^i$ = optimal node average flux in group g in instrumented node i,

$\phi_{g,cal}^i$ = calculated node average flux in group g in instrumented node i,

K_g^i = Kalman filter coefficient in group g $\left(= \dfrac{P H_g^i}{\sigma_m^2 + H_g^i P H_g^i}\right)$,

$A_{g,m}^i$ = measured activation rate in group g in instrumented node i,

P = calculation error,

H_g^i = conversion factor $\left(= \sigma_g \dfrac{\phi_{g,cal}^{i,det}}{\phi_{g,cal}^i}\right)$,

σ_m^2 = measurement error,

σ_g = detector cross section,

$\phi_{g,cal}^{i,det}$ = calculated detector average flux in group g in instrumented node i.

The calculated detector average fluxes and activation rates in Eq. (1) are determined by a local interpolation of the flux inside a node containing a detector.

2.2 Extrapolated Fluxes in the Core

For the core analysis we need to know the true flux distributions in every node in the core. We can obtain them in the instrumented nodes from the optimally estimated fluxes provided by the Kalman filter technique. However, we do not have them for the noninstrumented nodes. In COMPASS the extrapolated fluxes in noninstrumented nodes are obtained by combining the optimally estimated fluxes in instrumented nodes and the coupling coefficients which are calculated by the node average fluxes and outgoing currents provided by the three-dimensional nodal calculation.

The starting point for the derivation of a "Nodal Extrapolated Fluxes" is the two-group nodal equation:

$$\sum_{u=x,y,z} \frac{1}{a_u^m}\left[\left(j_{gul}^{-m} + j_{gur}^{+m}\right) - \left(j_{gul}^{+m} + j_{gur}^{-m}\right)\right] + \left(\Sigma_{ag}^m + \sum_{g'>g} \Sigma_{g\,g'}^m\right)\phi_g^m$$
$$= \sum_{g'<g} \Sigma_{g'\,g}^m\, \phi_{g'}^m + \frac{1}{\lambda}\sum_{g'} \chi_g\, \nu\Sigma_{fg'}^m\, \phi_{g'}^m \qquad (2)$$

In Eq. (2) a_g^m, Σ_g^m, ϕ_g^m, λ, χ_g and $j_{gus}^{\pm m}$ represent mesh size in direction u, average cross sections, fluxes, eigenvalue, prompt fission spectrum, and partial currents of the node m.

Eq. (2) can be transformed in a form which describes the coupling between instrumented and noninstrumented node average fluxes. By introducing spatial coupling coefficients γ_{gus}^m derived from the average fluxes $\phi_{g,cal}^m$ and currents $j_{gus,cal}^{\pm m}$ of the nodal solution, Eq. (2) can be casted into the form for the noninstrumented box m^k:

$$\sum_{\substack{u=x,y,z \\ m_l^k(u),m_r^k(u)}} \frac{1}{a_u^{m^k}}\left[\left(\gamma_{gul}^{m^k} + \gamma_{gur}^{m^k}\right)\phi_g^{m^k} - \gamma_{gur}^{m_l^k(u)}\, \tilde{\phi}_g^{m_l^k(u)} - \gamma_{gul}^{m_r^k(u)}\, \tilde{\phi}_g^{m_r^k(u)}\right] +$$
$$\left(\Sigma_{ag}^{m^k} + \sum_{g'>g} \Sigma_{g\,g'}^{m^k}\right)\phi_g^{m^k} = \sum_{g'<g} \Sigma_{g'\,g}^{m^k}\, \phi_{g'}^{m^k} + \frac{1}{\lambda}\sum_{g'} \chi_g\, \nu\Sigma_{fg'}^{m^k}\, \phi_{g'}^{m^k} \qquad (3)$$

where

$\phi_g^{m^k}$ = extrapolated flux for the noninstrumented node m^k,

$m_{l\,(r)}^k(u)$ = left (right) node adjacent to the non instrumented box m^k in the u-direction,

$\tilde{\phi}_g^{m_s^k(u)}$ = $\hat{\phi}_g^{m_s^k(u)}$, the optimally estimated flux for the instrumented node,

= $\phi_g^{m_s^k(u)}$, extrapolated flux for the noninstrumented node,

$\gamma_{gul}^m = j_{gul,cal}^{-m} / \phi_{g,cal}^m$,

$\gamma_{gur}^m = j_{gur,cal}^{+m} / \phi_{g,cal}^m$.

In the above equation we assumed that the spatial coupling coefficients of the best estimated state are equal to those of the diffusion theory calculation. Eq. (3) is solved for noninstrumented nodes by using the vectorized red-black Gauss-Seidel iteration scheme.

2.3 Cross Section Adjustment

In this section a nodal method is presented how the absorption cross sections (Σ_{a1}, Σ_{a2}), which are free parameters of the model, can be adjusted in a core such that a given flux map (extrapolated flux distribution) can be reproduced. This will coincide the system parameters with the core conditions with respect to the core eigenvalue and flux distributions. This type of nodal method is called the backward nodal solution method in the sense that cross sections are determined for given fluxes and eigenvalue. The results of this method are the absorption cross sections which form a consistent set of eigenvalue, currents and fluxes of the forward(normal) nodal solution. The adjusted cross sections are obtained by solving forward nodal solution iteratively.

The starting point for the derivation of the backward nodal solution is the two-group neutron diffusion equation in P_1form. With the partial currents, the extrapolated fluxes and cross sections, the free parameters (Σ_{a1}, Σ_{a2}) can be determined from the node neutron balance equation:

$$\Sigma_{a1}^{m} = \left(-L_1^m - \Sigma_{21}^m \phi_1^m + \frac{1}{\lambda}\sum_{g'} \nu\Sigma_{fg'}^m \phi_{g'}^m\right) / \phi_1^m,$$
$$\Sigma_{a2}^{m} = \left(-L_2^m + \Sigma_{21}^m \phi_1^m\right) / \phi_2^m, \qquad (4)$$

where

$$L_g^m = \sum_{u=x,y,z} \frac{1}{a_u^m}\left[\left(j_{gul}^{-m} + j_{gur}^{+m}\right) - \left(j_{gul}^{+m} + j_{gur}^{-m}\right)\right]. \qquad (5)$$

Since the partial currents and fluxes are related in nodal solution, Eqs. (4) and (5) are solved iteratively including thermal feedback effects on the cross section. For example, in the NEM (Nodal Expansion Method)[7] the outgoing partial currents on the left and right surfaces are given as functions of the diffusion coefficients, the incoming currents, the one-dimensional flux expansion coefficients (a_{3gu}, a_{4gu}) and the given nodal extrapolated fluxes.

$$j_{gul}^{-m} = c_{1gu}^m \left(\phi_g^m + a_{4gu}^m\right) + c_{2gu}^m j_{gul}^{+m} + c_{3gu}^m j_{gur}^{-m} - c_{4gu}^m a_{3gu}^m,$$
$$j_{gur}^{+m} = c_{1gu}^m \left(\phi_g^m + a_{4gu}^m\right) + c_{3gu}^m j_{gul}^{+m} + c_{2gu}^m j_{gur}^{-m} + c_{4gu}^m a_{3gu}^m, \qquad (6)$$

where

c_{igu}^m = constant determined from the diffusion coefficient and mesh size.

2.4 System Structure

A flow diagram of the overall structure of COMPASS is presented in Figure 1. In COMPASS the input such as core geometry, cross sections, derivatives of cross sections and core boundary conditions are transferred from the nuclear design code MASTER via the COMPASS data base file. COMPASS provides periodically its operation record file containing power history with MASTER for the detailed core follow calculation and receives its data base file.

III. Results

In order to ensure that COMPASS is capable of faithfully capturing the characteristics of the best estimate nuclear design code MASTER, its prediction uncertainty in power distribution has been evaluated and compared with that of COLSS using SMART Cycle 1 core configuration[8]. During power operation of SMART, three different control rod groups take charge of the core power control. The incore detectors consist of 20 radial detectors having 5 axial segments[9].

For the evaluation we set up a large number of power shapes from the data set of 105 actual power shapes, which cover the most of the spectrum of power profiles resulted from a power maneuvering simulation during core life. The 105 actual power shapes consist of three different axial xenon distributions (equilibrium, top and bottom peaked) at each of the seven power levels (105%, 100%, 90%, 80%, 70%, 60%, 50%) for the five burnup points (0, 300, 600, 900, 1050 EFPDs). These test cases include extremely skewed power shapes of which the axial offset (A.O.) is in the range of –50% to +50%.

The in-core detector signals are generated by the best estimate code MASTER and then inputted to both COMPASS and COLSS. COLSS synthesizes the core axial power distribution from the in-core detector power signals by a Fourier series method[10] and then generates a pseudo hot-pin power shape using the pre-calculated F_{xy} data generated by MASTER. The current COLSS uses the core maximum F_{xy} corresponding to each of control rod configurations. However, we also tested COLSS with the layer-wise F_{xy}'s for reducing the power prediction error coming from F_{xy} evaluation.

Figure 2 shows the comparison of the nominal core axial power shapes in BOC and EOC of SMART Cycle 1. The COLSS axial power shape agrees well with the reference at BOC but significantly deviates from the reference at EOC. The axial power peak F_z and the hot-pin F_q prediction errors are evaluated and summarized in Table 1. The COLSS results show a large deviation from the reference code MASTER. The rather large deviation results from the simple and conservative synthesis of core power distribution by Fourier series method and F_{xy} used in COLSS. The total uncertainties in COLSS F_z and F_q are estimated to be 4.29% and 3.72~5.78%, respectively. However, the COMPASS power prediction is exactly identical to MASTER. This means that the overall COMPASS uncertainty is the same as MASTER's peaking factor uncertainty[11] and that the additional penalty required for the uncertainty in peaking factor generation can be eliminated.

The overall computational time of COMPASS required for one time step adaptation (TIME in Fig. 1) is about 2.8 seconds on SUN ULTRA SPARCII-300 MHz. If we follow the same calculation period of current COLSS logic in which pseudo pin power distributions are synthesized every 10 seconds, COMPASS computational time is considered fast enough to produce them for on-line monitoring and surveillance.

IV. Conclusions

COMPASS has been developed and tested for the 105 actual power shapes of SMART. From the uncertainty evaluation results described in section III, the COMPASS peaking factor uncertainty is no more than that of the design code MASTER. However, current COLSS logic requires additional uncertainty of about 4% in the peaking factor for the same pseudo pin power measured. This bigger uncertainty in the COLSS peaking factor is due to the simple and conservative way of synthesizing the core power shapes, and in consequence it loses the thermal margin for core operation. In contrast, COMPASS eliminates the uncertainty involved in producing pseudo pin power peaking factor for the on-line core monitoring and it thus increases the thermal margin for core operation.

Acknowledgements

This project has been carried out under the Nuclear R&D Program by MOST.

References

1. Combustion Engineering Inc., “Overview Description of the Core Operation Limit Supervisory System (COLSS),” CEN-312-P, Revision 01-P, November 1986.
2. J. K. Seo, et al., “Advanced Integral Reactor (SMART) for Nuclear Desalination,” IAEA-SM-347/40, Proceedings of Symposium on Desalination of Seawater with Nuclear Energy, Taejon, Korea, May 1997.
3. J. Huesken and B. O. Cho, ”Specification of the Adaptive Core Model of COPS,” Work-Report KWU BT25/1992/251.
4. B. O. Cho et al., ”MASTER2.0 Methodology Manual,” KAERI/Technical Report to be published.
5. A. H. Jazwinski, ”Stochastic Process and Filtering Theory,” Academic Press, New York (1970).
6. B. O. Cho et al., “A highly Efficient Flux and Power Mapping Technique for Incore Detector Measurements, ”Proceedings of the International Conference on Mathematics and Computations, Reactor Physics, and Environmental Analyses, Portland, Oregon, Vol. 1, 652, April 30, 1995.
7. H. Finnemann, H, Raum, “Nodal Expansion Method for the Analysis of Spacetime Effects in LWRs,” Proceedings of a Specialists' Meeting on Calculation of 3Dimensional Rating Distributions in Operating Reactors, Paris, November 1979.
8. C. C. Lee et al., ”Nuclear Design Characteristics of SMART,” Proceedings of the Korean Nuclear Society Spring Meeting, Volume 1, Seoul, Korea, May 1988.
9. K. B. Lee, “Determination of Incore Detector Location for SMART Core,” SMART-CA-CA110-07 Rev. 01, January 1, 1998.
10. Combustion Engineering Inc., “Assessment of the Accuracy of PWR Operation Limits as Determined by the Core Operation Limit Supervisory System (COLSS),” CENPS-D-169-P, July 1975.
11. J. S. Song et al., ”Verification and Uncertainty Evaluation of CASMO-3/MASTER Nuclear Analysis System,” KAERI/TR-806/97, Jan. 1997.

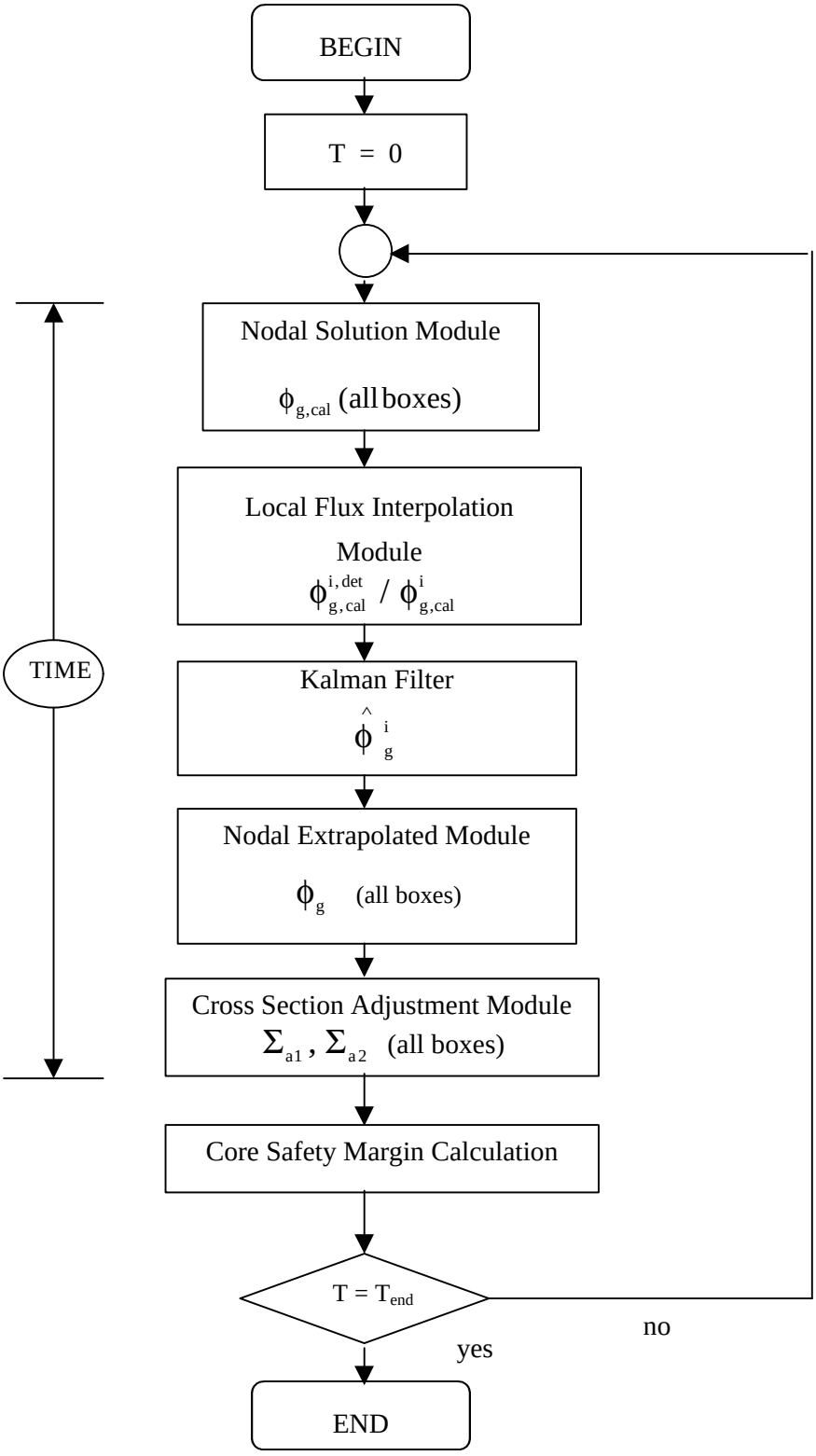

Figure 1. Flow Diagram of the Calculation Procedure of COMPASS

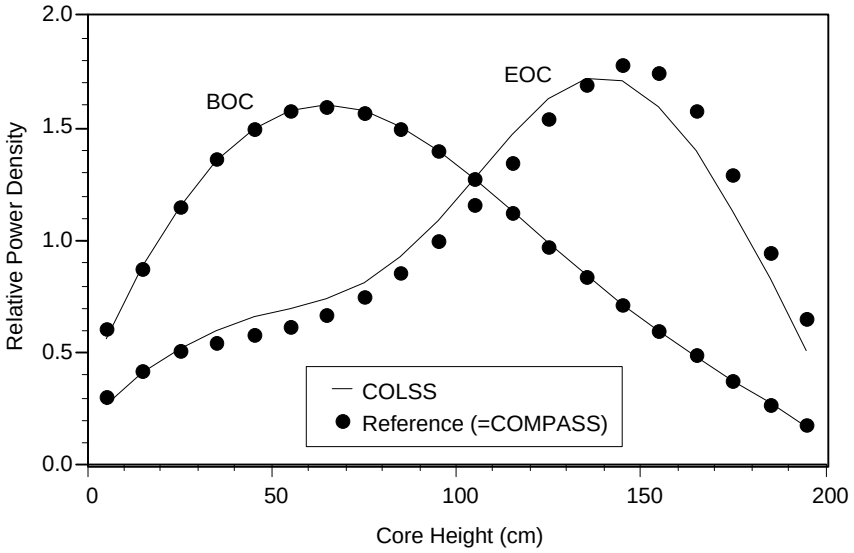

Figure 2. Comparison of Nominal Axial Power Shapes for SMART Cycle 1

Table 1. Comparison of F_z and F_q Prediction Error

		Average (%)	STD (%)	TL[(a)] (%)
COLSS	F_z	0.27	2.71	4.29*
	F_q	15.57(1)	5.83	5.78**
		2.78(2)	3.87	3.72**
COMPASS	F_z	0.00	0.00	0.00
	F_q	0.00	0.00	0.00

$$F_{z(q)} \text{ Prediction Error} = \left[\frac{F_{z(q)\ \text{COLSS(COMPASS)}} - F_{z(q)\ \text{MASTER}}}{F_{z(q)\ \text{MASTER}}} \right] x\,100\,(\%)$$

(a) 95/95 Tolerance Limit

(1) Maximum F_{xy} used

(2) Layer-wise F_{xy} used

* Upper Tolerance Limit

** Lower Tolerance Limit